JCB Article

A cryptic fragment from fibronectin's III1 module localizes to lipid rafts and stimulates cell growth and contractility

Denise C. Hocking and Katherine Kowalski

Department of Pharmacology and Physiology, University of Rochester Medical Center, Rochester, NY 14642

The interaction of cells with the extracellular matrix (ECM) form of fibronectin (FN) triggers changes in growth, migration, and cytoskeletal organization that differ from those generated by soluble FN. As cells deposit and remodel their FN matrix, the exposure of new epitopes may serve to initiate responses unique to matrix FN. To determine whether a matricryptic site within the III1 module of FN modulates cell growth or cytoskeletal organization, a recombinant FN with properties of matrix FN was constructed by directly linking the cryptic, heparin-binding COOH-terminal fragment of III1 (III1H) to the integrin-binding III8–10 modules (glutathione-*S*-transferase [GST]–III1H,8–10). GST–III1H,8–10 specifically stimulated increases in cell growth and contractility; integrin ligation alone was ineffective. A construct lacking the integrin-binding domain (GST–III1H,2–4) retained the ability to stimulate cell contraction, but was unable to stimulate cell growth. Both GST–III1H,2–4 and matrix FN colocalized with caveolin and fractionated with low-density membrane complexes by a mechanism that required heparan sulfate proteoglycans. Disruption of caveolae inhibited the FN- and III1H-mediated increases in cell contraction and growth. These data suggest that a portion of ECM FN partitions into lipid rafts and differentially regulates cytoskeletal organization and growth, in part, through the exposure of a neoepitope within the conformationally labile III1 module.

Introduction

Fibronectins are a family of multidomain glycoproteins that are deposited in the extracellular matrix (ECM)* where they promote adhesive and migratory events (Hynes, 1990). The polymerization of soluble fibronectin (FN) into insoluble fibrils within the ECM is a dynamic, cell-dependent process that is mediated by a series of events involving the actin cytoskeleton and integrin receptors (Magnusson and Mosher, 1998). Studies indicate that the interaction of cells with the ECM form of FN triggers changes in cell cycle progression, cell migration, and cytoskeletal organization that differ from those generated by the interaction of cells with nonpolymerized FN (Morla et al., 1994; Sottile et al., 1998; Sechler and Schwarzbauer, 1999; Hocking et al., 2000). Other studies suggest that FN polymers formed in vitro have antimetastatic (Pasqualini et al., 1996) and antiangiogenic properties (Yi and Ruoslahti, 2001). The mechanism by which the ECM form of FN gives rise to cellular phenotypes distinct from soluble FN is not known.

Current models of FN matrix assembly propose that binding of soluble FN to the cell surface triggers a series of conformational changes that result in the exposure of homophilic binding sites and the subsequent elongation of FN fibrils (Magnusson and Mosher, 1998). The first type III module of FN (III1) contains a binding site for the NH_2 terminus of FN that is not exposed within soluble FN (Hocking et al., 1994), but may become exposed on cell surfaces during FN polymerization (Zhong et al., 1998; Tellier et al., 2000). Moreover, proteolytic cleavage of III1 at Ile597 exposes a cryptic heparin-binding activity in III1 (Litvinovich et al., 1992). These data suggest the possibility that during FN polymerization, a "matricryptic" (Davis et al., 2000), heparin-binding activity is exposed in III1, which serves to trigger cellular responses that are unique to ECM FN.

Previous work has shown that FN stimulates cell growth (Sottile et al., 1998) and contractility (Hocking et al., 2000) by a mechanism that requires the polymerization of FN into the ECM. To construct a recombinant FN with properties of matrix FN, we engineered a glutathione-*S*-transferase (GST)– tagged fusion protein in which the cryptic, heparin-binding III1 fragment (III1H) was linked directly to the inte-

Address correspondence to Denise C. Hocking, Department of Pharmacology and Physiology, University of Rochester Medical Center, 601 Elmwood Ave., Box 711, Rochester, NY 14642. Tel.: (716) 273-1770. Fax: (716) 273-2652. E-mail: denise_hocking@urmc.rochester.edu

*Abbreviations used in this paper: ECM, extracellular matrix; FN, fibronectin; GST, glutathione-*S*-transferase; HSPGs, heparan sulfate proteoglycans.

Key words: fibronectin; caveolin; integrin; proteoglycans; growth

grin-binding III8–10 modules (GST–III1H,8–10). FN-null ($FN^{-/-}$) cells, which do not produce FN and are grown under serum-free conditions (Sottile et al., 1998), were used in conjunction with recombinant FN fragments to eliminate any effects of endogenous FN or FN fragments. Our data indicate that treatment of $FN^{-/-}$ cells with GST–III1H,8–10 stimulates a specific increase in cell growth and contractility. A construct in which the III2–4 modules were substituted for the integrin-binding III8–10 modules (GST–III1H,2–4) retained the ability to stimulate cell contraction, but did not stimulate cell growth. Both GST–III1H,2–4 and polymerized FN colocalized with caveolin and fractionated with low-density membrane complexes by a mechanism that required heparan sulfate proteoglycans (HSPGs). Treatment of cells with sterol-binding compounds to disrupt caveolae blocked the localization of GST–III1H,2–4 and FN to lipid rafts and inhibited the increase in cell contraction and growth induced by either FN or the III1H-containing constructs. These data suggest that a portion of ECM FN partitions into lipid rafts and differentially regulates cytoskeletal organization and cell growth, in part, through the exposure of a neoepitope within the conformationally labile III1 module.

Results

A cryptic fragment of III1 stimulates cell growth

In the absence of FN, $FN^{-/-}$ cells that are adherent to type I collagen exhibit a typical cell doubling rate of 20 h (Sottile et al., 1998). Addition of GST–III1H,8–10 to collagen-adherent $FN^{-/-}$ cells stimulated a dose-dependent increase in cell growth compared with untreated cells (Fig. 1 A). Substitution of the heparin-binding III13 module (Bloom et al., 1999) for III1H (GST–III8–10,13) did not stimulate cell growth (Fig. 1 A). Treatment of cells with an FN construct in which the III2–4 modules were substituted for the III8–10 modules also did not increase cell growth (Fig. 1 A), suggesting that integrin ligation is necessary for the growth response to GST–III1H,8–10. However, treatment of cells with integrin-binding constructs in which the III1H fragment was absent (GST–III8–10 and GST–III9–10), or in which the corresponding COOH-terminal III2 fragment (III2H) was substituted for III1H (GST–III2H,8–10) failed to increase cell growth (Fig. 1 B), suggesting that III1H is also required. Cell growth was not increased when individually expressed GST–III1H was added to cells either alone or in combination with GST–III8–10 (GST–III1H + GST–III8–10; Fig. 1 B), suggesting that clustering of cell surface–bound III1H by binding of III8–10 to integrin receptors (Hynes, 1990) may be important for its activity.

To further define the role of III1H, $FN^{-/-}$ cells were treated with GST–III1H,8–10 in the absence and presence of increasing concentrations of GST–III1H. As shown in Fig. 2 A, GST–III1H,8–10-stimulated growth was inhibited by coincubation of cells with the III1H fragment. In contrast, GST–III1H,8–10-stimulated growth was not inhibited when cells were coincubated with the fragment of III2 corresponding to the III1H truncation (GST–III2H; Fig. 2 A). GST–III1H,8–10-stimulated growth was also inhibited by addition of the integrin-binding constructs GST–III8–10 and GST–III9–10 (Fig. 2 B). Moreover, mutation of the integrin synergy site (GST–III9–$10^{R1374,1379A}$) (Aota et al., 1994) suppressed the ability of GST–III9–10 to inhibit GST–III1H,8–10 growth (Fig. 2 B), further demonstrating a role for integrin ligation in the growth response to GST–III1H,8–10.

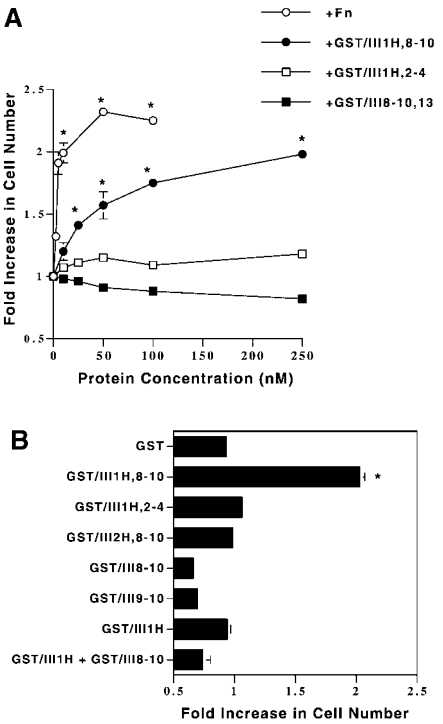

Figure 1. **Effect of GST–III1H,8–10 on cell growth.** $FN^{-/-}$ cells were seeded on collagen-coated wells. 4 h after seeding, cells were treated with increasing concentrations of either intact FN (+Fn, ○), GST–III1H,8–10 (●), GST–III1H,2–4 (□), or GST–III8–10,13 (■). In B, cells were treated with 250 nM of the various recombinant proteins. 4 d after seeding, cell number was determined as described in the Materials and methods. Data are presented as fold increase in cell number over control (growth in the absence of additional protein). *Significantly different from control, $P < 0.001$.

Heparin-binding activity is required for increased growth

The ability of GST–III1H,8–10 to bind to heparin was assessed in solid phase binding assays. As shown in Fig. 3 A, GST–III1H,8–10 bound biotin-labeled heparin, whereas GST–III8–10 did not. Heparin-binding activity was also observed with GST–III8–10,13 and was greater than that observed with GST–III1H,8–10 (Fig. 3 A). The heparin-binding activity of GST–III8–10,13 was similar to that observed with the FN construct that contains both the III12 and III13 modules (GST–III12–13) (Fig. 3 A). Control studies indicated that an equal amount of fusion protein bound in each well (unpublished data).

To determine whether the heparin-binding activity of III1H plays a role in GST–III1H,8–10-stimulated growth, cells were incubated with GST–III1H,8–10 in the absence and presence of either sulfated or nonsulfated heparin. Coincubation with sulfated heparin, but not nonsulfated heparin, reduced GST–III1H,8–10 growth to control levels (Fig. 3 B). Similarly, treatment with heparinase I inhibited the growth response to GST–III1H,8–10 by ~50%, suggesting a role for HSPGs (Fig. 3 C). Heparinase treatment had no effect on control cell growth (Fig. 3 C). To determine whether other known heparin-bind-

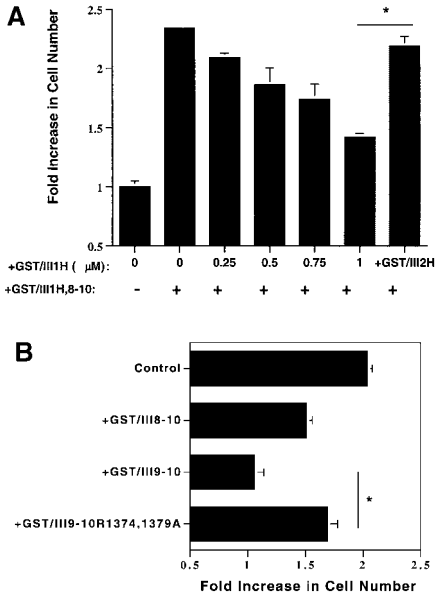

Figure 2. **Role of III1H and III9–10 in GST–III1H,8–10-stimulated growth.** $FN^{-/-}$ cells were seeded as in the legend to Fig. 1. In A, cells were treated with 250 nM GST–III1H,8–10 in the absence (0) and presence of GST–III1H or 1 μM GST–III2H. *+GST–III1H (1 μM) differs significantly from +GST–III2H, $P < 0.01$. In B, cells were treated with 100 nM GST–III1H,8–10 in the absence (control) and presence of either 1 μM GST–III8–10, GST–III9–10, or GST–III9–$10^{R1374,1379A}$. Cells were processed as indicated in the legend to Fig. 1. *+GST–III9–$10^{R1374,1379A}$ differs significantly from +GST–III9–10, $P < 0.01$.

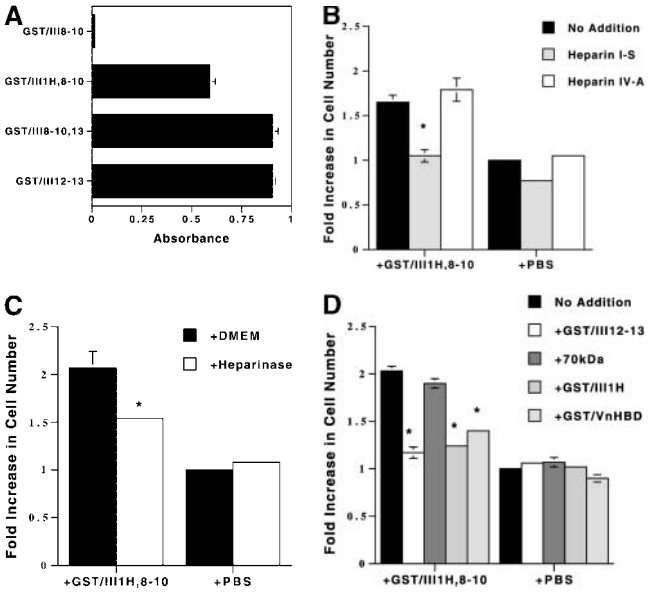

Figure 3. **Role of heparin-binding activity in GST–III1H,8–10 growth.** (A) Glutathione-coated plates were incubated with saturating concentrations of the various fusion proteins. Binding of biotin–heparin was assayed by EIA. Data represent the mean absorbance of triplicate wells ± SD. In B–D, $Fn^{-/-}$ cells were seeded as indicated in the legend to Fig. 1. After 4 h, cells were treated with 100 nM GST–III1H,8–10 or an equal volume of PBS. In B, cells were coincubated with 50 μM sulfated (heparin I-S) or nonsulfated (heparin IV-A) heparin. *Significantly different from +GST–III1H,8–10, $P < 0.001$. In C, cells were pretreated with heparinase I or an equal volume of DME. *Significantly different from +GST–III1H,8–10, $P < 0.05$. In D, cells were coincubated with 1 μM of the various heparin-binding fragments. *Significantly different from GST–III1H,8–10 alone, $P < 0.001$.

ing domains could compete with the growth-promoting effects of GST–III1H,8–10, $FN^{-/-}$ cells were incubated with GST–III1H,8–10 in the absence and presence of various heparin-binding fragments. As shown in Fig. 3 D, addition of a 10-fold excess of either GST–III1H, GST–III12–13, or GST–Vn-HBD inhibited the cell growth response to GST–III1H,8–10. In contrast, addition of the NH_2-terminal 70-kD fragment had little effect on GST–III1H,8–10-stimulated growth. Addition of the heparin-binding domains to control cells had no effect on basal cell growth (Fig. 3 D). Taken together, these data suggest that the heparin-binding activity of III1 is necessary for the stimulation of cell growth.

Effect of III1H on cell contractility

FN polymerization has also been shown to trigger cytoskeletal tension generation (Hocking et al., 2000). To determine the role of III1H in cell contractility, $FN^{-/-}$ cells were imbedded in floating collagen gels in the absence and presence of increasing concentrations of either intact FN or the various fusion proteins. GST–III1H,8–10 stimulated an increase in cell contractility to a similar extent as that observed with intact FN (Fig. 4 A). Furthermore, in contrast to the negative results obtained in the growth studies, treatment of cells with GST–III1H,2–4 also promoted a significant increase in collagen gel contraction (Fig. 4 A). As with the growth assays, substitution of the heparin-binding III13 module for III1H (GST–III8–10,13) failed to stimulate collagen gel contraction (Fig. 4 A). Addition of the III1H fragment resulted in a dose-dependent inhibition of GST–III1H,8–10-induced contraction; intact III1 had no effect (Fig. 4 B). Moreover, treatment of cells with GST–III1–4, in which III1H was replaced with the intact III1 module, did not stimulate contraction (Fig. 4 C), suggesting that exposure of cryptic residues within III1 is required to induce cytoskeletal tension generation. Constructs in which one or more of the COOH-terminal type III modules were deleted (GST–III1H,2–3, GST–III1H,2, and GST–III1H) did not stimulate cell contractility (Fig. 4 C), suggesting that secondary sequences contribute to the ability of III1H to stimulate contraction. These data suggest that a cryptic, heparin-binding region within the III1 module of FN plays a unique role in modulating both cell contractility and growth.

GST–III1H,8–10 does not localize to focal contacts

To explore the mechanism by which the III1H constructs stimulate growth and contractility, studies were conducted to determine whether GST–III1H,2–4 and GST–III1H,8–10 localize to specific cell surface structures. Collagen-adherent $FN^{-/-}$ cells were treated with the various fusion proteins and then examined by immunofluorescence microscopy for GST to visualize the fusion proteins, and for vinculin, a marker of focal adhesions (Jockusch et al., 1995). As shown in Fig. 5, staining of GST–III1H,2–4 (Fig. 5 A, arrow) and GST–III1H,8–10 (Fig. 5 B, arrow) was detected in discrete clusters that did not colocalize with vinculin (Fig. 5, E and F). In contrast, GST–III8–10,13 staining strongly colocalized with vinculin (Fig. 5, C, G, and K, arrows) in a pattern similar to that observed with GST–III8–10 (unpublished

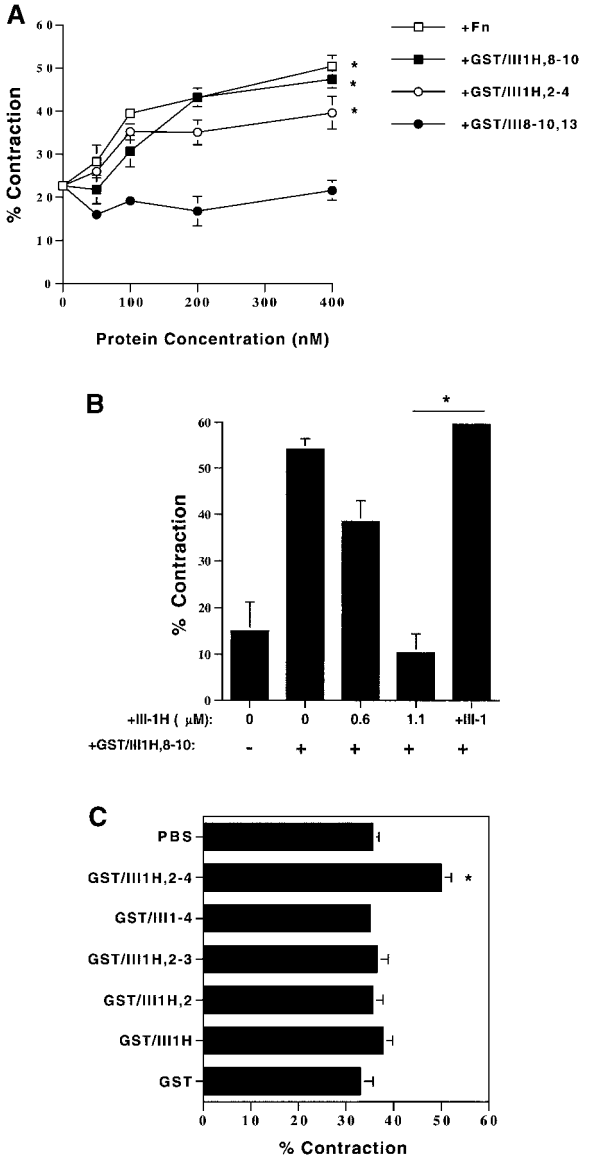

Figure 4. **GST–III1H,2–4 stimulates cell contraction.** $FN^{-/-}$ cells were mixed with neutralized type I collagen in the presence of (A) increasing concentrations of intact FN (+Fn, □), GST–III1H,8–10 (■), GST–III1H,2–4 (○), or GST–III8–10,13 (●). *Significantly different from contraction in the absence of additional protein, $P < 0.001$. In B, 250 nM GST–III1H,8–10 was added to gels in the absence (0) and presence of increasing concentrations of III1H or 1 μM III1. *The addition of III1H (1.1 μM) is significantly different from +III1, $P < 0.01$. In C, 250 nM fusion protein or an equal volume of PBS was added to cells. *Significantly different from +PBS, $P < 0.001$. Cell–collagen mixtures were polymerized as described in the Materials and methods.

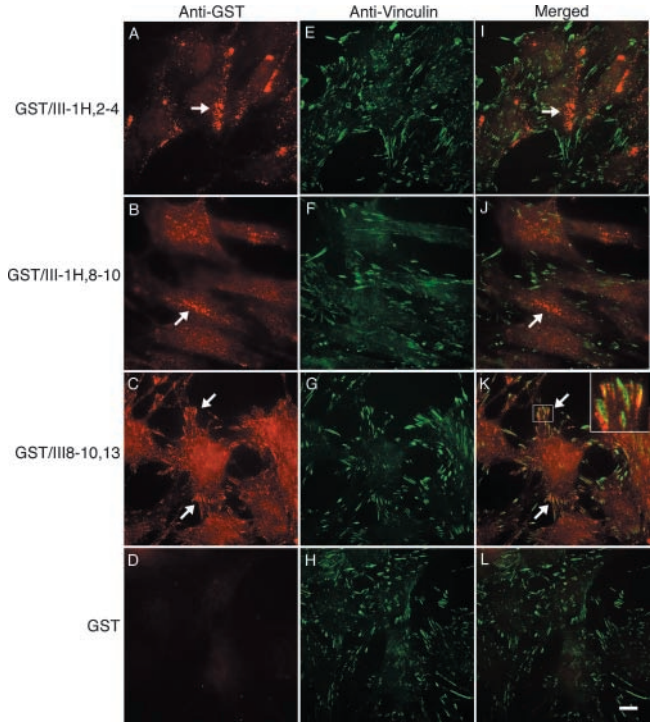

Figure 5. **Localization of III1H constructs on cell surfaces.** Collagen-adherent $Fn^{-/-}$ cells were incubated with 250 nM of GST–III1H,2–4 (A, E, and I), GST–III1H,8–10 (B, F, and J), GST–III8–10,13 (C, G, and K), or GST (D, H, and L). Cells were processed for immunofluorescence as indicated in the Materials and methods. Fusion proteins were visualized using a polyclonal anti-GST antibody followed by a Texas red–labeled goat anti–rabbit antibody (A–D). Vinculin was visualized using an antivinculin mAb followed by an FITC-labeled goat anti–mouse antibody (E–H). In the merged images shown in I–L, areas of colocalization appear yellow. Bar, 10 μM.

data). No staining was observed when cells were treated with GST alone (Fig. 5 D).

GST–III1H,2–4 colocalizes with caveolin by an HSPG-dependent mechanism

To further identify the structures in which the III1H constructs localized, cells were incubated with either GST–III1H,2–4 or GST and examined by immunofluorescence microscopy for GST and caveolin, a marker of cell surface membrane invaginations, termed caveolae (Anderson, 1998). As shown in Fig. 6, GST–III1H,2–4 staining (Fig. 6 A, arrows) colocalized with caveolin staining (Fig. 6, B and C, arrows). When cells were treated with GST alone, GST staining was not observed (Fig. 6 D), whereas caveolin staining was still detected (Fig. 6 E, arrow). Pretreatment of cells with filipin III, which binds cholesterol and disrupts caveolae (Anderson, 1998), caused a concomitant decrease in both GST–III1H,2–4 and caveolin staining (Fig. 6, G and H). Filipin III did not disrupt cell adhesion, as cells treated with filipin III remained well spread (Fig. 6 I).

To determine whether the cell surface localization of GST–III1H,2–4 was dependent upon HSPGs, collagen-adherent $FN^{-/-}$ cells were pretreated with heparinase before the addition of GST–III1H,2–4. As shown in Fig. 7 A, clustering of GST–III1H,2–4 on the cell surface was abolished by pretreatment with heparinase. In contrast, pretreatment of cells with either chondroitinase ABC (Fig. 7 a, C) or neuraminidase (Fig. 7 a, D) had no effect on the cell surface staining of GST–III1H,2–4. Heparinase treatment did not affect cell adhesion, as demonstrated by vinculin staining of focal adhesions (Fig. 7 a, F).

Proteins associated with caveolae are resistant to solubilization by either Triton X-100 or high pH carbonate buffer and can be purified by flotation on sucrose gradients (Schwab et al., 2000). To determine whether GST–III1H,2–4 associates with low-density membrane complexes by a mechanism that is dependent upon HSPGs, collagen-adherent $FN^{-/-}$ cells

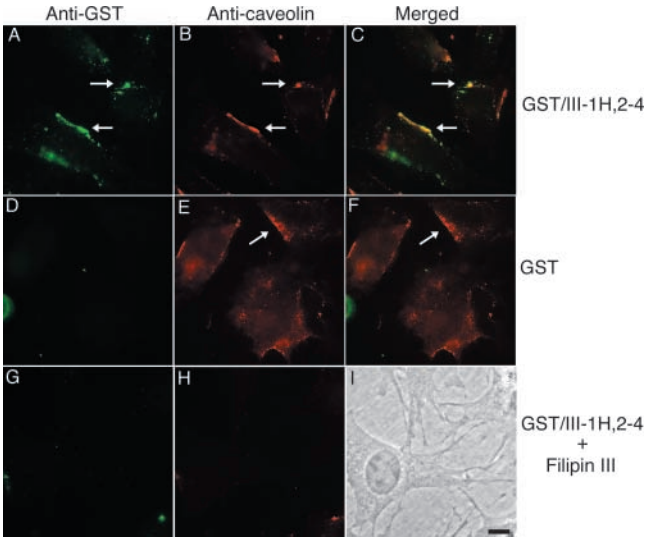

Figure 6. **Colocalization of GST–III1H,2–4 with caveolin.** Collagen-adherent $FN^{-/-}$ cells were incubated with 250 nM of GST (D, E, and F) or GST–III1H,2–4 in the absence (A, B, and C) and presence of 2.5 μg/ml filipin III (G, H, and I). Cells were then processed for immunofluorescence. Fusion proteins were visualized using an anti-GST mAb followed by an FITC-labeled goat anti–mouse antibody (A, D, and G). Caveolin was visualized using a polyclonal anticaveolin antibody followed by a Texas red–labeled goat anti–rabbit antibody (B, E, and H). In the merged images shown in C and F, areas of colocalization appear yellow. The phase contrast image of cells treated with GST–II-1H,2–4 and filipin III is shown in I. Bar, 10 μM.

were pretreated with heparinase I or an equivalent volume of DME, before the addition of GST–III1H,2–4. Cells were extracted with 1% Triton X-100 and fractionated by high-speed centrifugation. Under these conditions, the majority of cellular protein remains associated with the high-density sucrose (Fig. 7 b, fractions 9–12); proteins associated with low-density lipids are buoyant and rise to the interface of the 5 and 30% sucrose layers (Schwab et al., 2000). As previously demonstrated, both caveolin and β-actin, but not LAMP-1, associate with low-density membrane domains and thus migrate to the interface of the 5 and 30% sucrose layers (Fig. 7 b, fractions 5 and 6) (Anderson, 1998). GST–III1H,2–4 also comigrated to these low-density membrane fractions (Fig. 7 b, fractions 5 and 6). Moreover, pretreatment of cells with heparinase significantly reduced the amount of GST–III1H,2–4 associated with the low-density lipid complexes (Fig. 7 b). In contrast, heparinase treatment had no effect on the association of either caveolin or β-actin with low-density lipid complexes (Fig. 7 b). These data suggest that GST–III1H,2–4 localizes to caveolin-enriched membrane domains by an HSPG-dependent mechanism. GST–III1H,8–10 was also detected in the caveolin-enriched fractions, whereas GST–III8–10,13 was not (Fig. 7 c), providing further evidence that III1H mediates the localization of these FN fragments to lipid rafts.

Partitioning of FN to lipid rafts requires FN polymerization and HSPGs

To determine whether intact FN also colocalizes with caveolin, confluent $FN^{-/-}$ cells were incubated with FN for 4 h. Cells were costained for FN and caveolin. As demonstrated in Fig. 8 a, areas of FN (Fig. 8 a, A, arrow) and caveolin (Fig. 8 a,

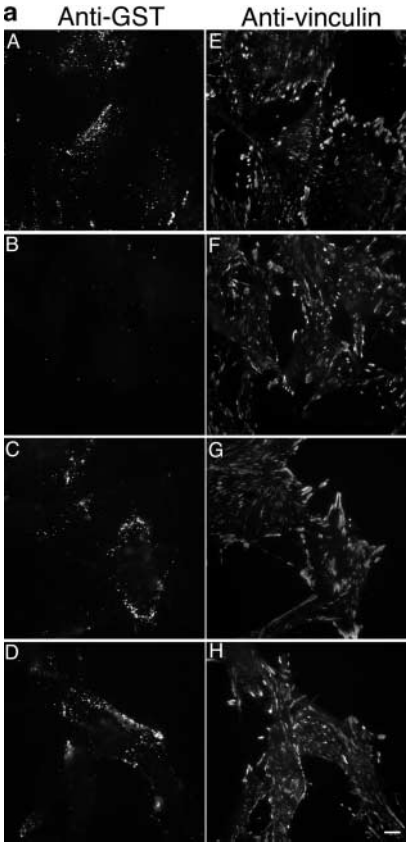

Figure 7. **Effect of heparinase on the localization of GST–III1H2–4 to caveolin-enriched lipid rafts.** (a) Collagen-adherent $FN^{-/-}$ cells were pretreated with either heparinase I (B and F), chondroitinase ABC (C and G), neuraminidase (D and H), or an equal volume of DME (A and E) before the addition of 250 nM GST–III1H,2–4. Staining for GST (A–D) and vinculin (E–H) was conducted as in the legend to Fig. 5. Bar, 10 μM. (b) Confluent $Fn^{-/-}$ cells were treated with either heparinase I or DME, before the addition of 250 nM GST–III1H,2–4. (c) Cells were incubated with 250 nM GST–III1H,8–10 or GST–III8–10,13. Cell lysates were fractionated by sucrose density gradient centrifugation, as described in the Materials and methods. Aliquots (120 μl) of each fraction were analyzed by PAGE and immunoblotting. GST–III1H,2–4 was identified using anti-FN mAb clone CCBD that recognizes an epitope in III4. The blot was then stripped and reprobed for LAMP-1. A separate immunoblot containing 5 μl of each fraction was analyzed for caveolin followed by β-actin. GST–III1H,8–10 and GST–III8–10,13 were identified using an anti-GST monoclonal antibody. Molecular mass markers are indicated to the left.

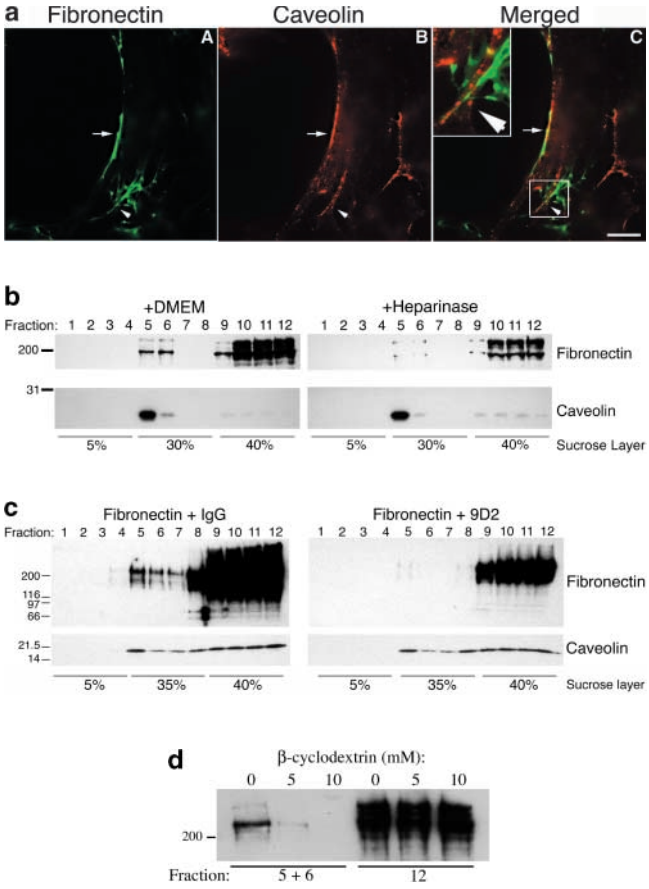

Figure 8. **Localization of FN to caveolin-enriched domains.** (a) Vitronectin-adherent $FN^{-/-}$ cells were incubated with 40 nM FN for 5 h. FN was visualized using a monoclonal anti-FN antibody followed by an FITC-labeled goat anti–mouse antibody (A). Caveolin staining is shown in B. The merged image appears in C. Bar, 10 μM. (b) Confluent $FN^{-/-}$ cells were treated with heparinase III or an equal volume of DME for 1 h followed by 40 nM FN for an additional 5 h. Cells were extracted with 1% Triton X-100 and analyzed by sucrose density gradient centrifugation followed by immunoblotting for either FN (120 μl fraction/lane) or caveolin (5 μl fraction/lane). (c) Confluent $FN^{-/-}$ cells were treated for 18 h with 20 nM FN in the presence of either nonimmune mouse IgG or 9D2 IgG. Cells were extracted with sodium carbonate buffer and fractionated by sucrose density gradient centrifugation. Aliquots of each fraction were analyzed by PAGE and immunoblotting using anti-FN and anticaveolin antibodies. (d) FN-null cells were incubated with 20 nM FN for 18 h and then incubated in the absence (0) or presence of either 5 or 10 mM cyclodextrin for 2 h. Cell extracts were separated by sucrose density gradient centrifugation and fractions 5 and 6 (corresponding to the low-density lipid fractions) were combined. Aliquots of both the combined fractions and fraction 12 (Triton X-100 soluble) were analyzed for FN by immunoblotting. Molecular mass markers are indicated to the left.

B, arrow) were found to colocalize (Fig. 8 a, C, arrow), particularly along cell edges. In addition, discrete areas of FN fibril staining appeared to terminate at areas enriched with caveolin (arrowhead). To determine whether the localization of FN to caveolin-enriched lipid rafts is similarly dependent on HSPGs, $FN^{-/-}$ cells were pretreated with heparinase before incubation with FN. After 5 h, cells were extracted with 1% Triton X-100 and fractionated. As shown in Fig. 8 b, a portion of the FN from untreated cells migrated to the caveolin-enriched fractions (fractions 5 and 6). Pretreatment of cells with heparinase significantly reduced the amount of FN associated with these fractions (Fig. 8 b, fractions 5 and 6).

To determine whether the localization of FN to caveolin-enriched lipid rafts requires FN polymerization, FN-null cells were treated with FN in the presence of either control mouse IgG or the anti-FN mAb, 9D2. The 9D2 mAb recognizes an epitope within the III1 module of FN and inhibits FN polymerization, but does not block the initial association of soluble FN with cell surfaces (Chernousov et al., 1991). After an 18-h incubation, cells were extracted using a high pH carbonate buffer and fractionated. As shown in Fig. 8 c, when FN polymerization was inhibited by the 9D2 mAb, FN staining was not detected in the low-density fractions (Fig. 8 c, fractions 5–8).

β-Cyclodextrin removes cholesterol from cell membranes and alters the association of proteins with caveolae (Keller and Simons, 1998). To determine whether disruption of caveolae would disrupt the association of FN with low-density lipid rafts, cells were allowed to polymerize an FN matrix and then were treated with cyclodextrin for 2 h. As shown in Fig. 8 d, cyclodextrin preferentially removed the FN associated with the low-density lipid fractions (fractions 5 and 6); cyclodextrin had no effect on the interaction of nonlipid-associated FN with cells (Fig. 8 d, fraction 12). Taken together, these data indicate that a portion of matrix FN partitions to lipid rafts by a mechanism that requires HSPGs.

III1H-mediated growth and contractility are inhibited by sterol-binding agents

To determine whether the fraction of GST–III1H,2–4 and FN that associates with caveolae is biologically active, $Fn^{-/-}$ cells were pretreated with the cholesterol-binding compounds nystatin and filipin III. Cells were then embedded in collagen gels in the presence of either FN or GST–III1H,2–4 and collagen gel contraction was assessed. As demonstrated in Fig. 9 A, pretreatment of cells with nystatin inhibited the contraction induced by GST–III1H,2–4 and partially inhibited the contraction induced by FN. In contrast, basal contraction was not altered by nystatin treatment (Fig. 9 A). A similar inhibition profile was obtained when cells were pretreated with filipin III (Fig. 9 B).

Studies were also conducted to determine whether disruption of caveolae inhibits GST–III1H,8–10- and FN-induced cell growth. Pretreatment of cells with nystatin inhibited the increase in cell growth induced by GST–III1H,8–10 and partially inhibited the increase in cell growth induced by intact FN (Fig. 9 C). Nystatin did not significantly affect basal cell growth (Fig. 9 C, +PBS). Pretreatment of cells with cyclodextrin also inhibited GST–III1H,8–10- and FN-stimulated growth while having no effect on basal growth (Fig. 9 D). Taken together, these data suggest that the ability of the heparin-binding fragment of III1 to stimulate cell contractility and growth is dependent upon its localization to caveolin-containing lipid rafts.

Discussion

Although the ECM form of FN is thought to be the primary functional form in vivo (Hynes, 1990), studies to date have focused primarily on the effects of soluble FN on cell func-

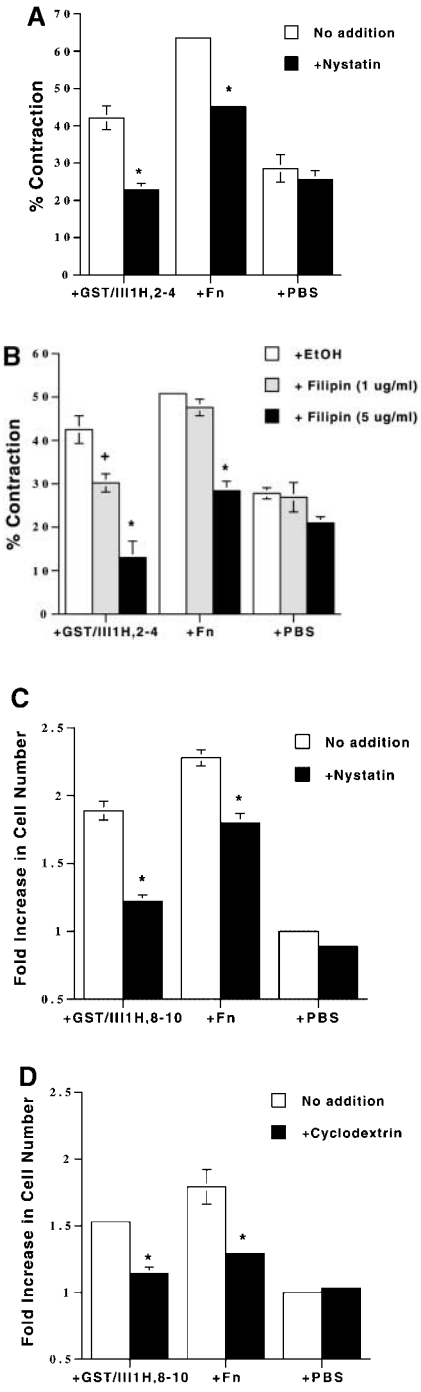

Figure 9. **Effect of cholesterol-binding agents on cell growth and contraction.** $Fn^{-/-}$ cells were imbedded into collagen gels, as indicated in the legend to Fig. 4, in the presence of either 250 nM GST–III1H,2–4, 50 nM FN (+Fn), or an equal volume of PBS. In A, some gels received 50 μg/ml nystatin. *Significantly different from the corresponding no addition, $P < 0.01$. In B, some gels received filipin III or an equal volume of ethanol (EtOH). $^{+}$Significantly different from +GST–III1H,2–4, $P < 0.01$. *Significantly different from +GST–III1H,2–4, $P < 0.001$. Collagen gels were cast and processed as indicated in the legend to Fig. 4. In C and D, collagen-adherent, $FN^{-/-}$ cells were treated with (C) 50 μg/ml nystatin or (D) 2 mM cyclodextrin. Cells were then incubated with either 100 nM of GST–III1H,8–10, 40 nM FN (+Fn), or an equal volume of PBS. 3 d after seeding, cells were processed as indicated in the legend to Fig. 1. *Significantly different from the corresponding no addition, $P < 0.01$.

tion. Recent studies indicate that the interaction of cells with matrix FN triggers changes in cell behavior that are distinct from those generated by the interaction of cells with soluble FN (Morla et al., 1994; Sottile et al., 1998; Sechler and Schwarzbauer, 1999; Hocking et al., 2000). The ability of FN constructs containing the cryptic heparin-binding region of III1 to stimulate cell growth and contractility suggests that one mechanism by which matrix FN gives rise to distinct cellular phenotypes is through the exposure of a neoepitope within III1 during FN matrix deposition or remodeling. Both the III1H-containing constructs, as well as intact FN, colocalized with caveolin and fractionated with caveolin-enriched membrane domains by a mechanism that required HSPGs. Moreover, localization of FN to caveolin-enriched fractions was blocked by an inhibitor of FN polymerization, suggesting that the matrix form of FN specifically translocates to lipid rafts. In addition, disruption of caveolae inhibited both the localization and the cellular responses to the III1H constructs and intact FN. Taken together, these data suggest that during ECM remodeling, a portion of matrix FN partitions into lipid rafts and differentially regulates cytoskeletal organization and cell growth, in part, through the exposure of a matricryptic, heparin-binding site within the III1 module.

The loss of lipid-associated FN upon treatment of cells with the inhibitor of FN polymerization, 9D2 mAb (Chernousov et al., 1991), suggests that the association of FN with lipid rafts occurs as FN is either assembled or remodeled within the ECM. Furthermore, the cholesterol-binding compound nystatin does not inhibit FN matrix deposition (unpublished data). These data suggest that the formation of an FN matrix does not depend on FN localization to lipid rafts. Rather, these data indicate that as a consequence of FN matrix deposition, a portion of the matrix FN translocates to lipid rafts where it modulates cell function. In support of this, previous work has shown that cell cycle progression is altered in cells that have assembled a matrix consisting of an FN construct in which modules III1–7 were deleted (Sechler and Schwarzbauer, 1998).

Previous studies have demonstrated that treatment of cells with an isolated fragment of III1, termed III1C (NH_2 terminus = Asn^{600}), inhibits lysophosphatidic acid–mediated actin organization and tyrosine phosphorylation (Bourdoulous et al., 1998), decreases cell migration (Morla et al., 1994), and inhibits tumor cell angiogenesis (Yi and Ruoslahti, 2001). The ability of III1C to affect cytoskeletal function has been attributed to its ability to either disrupt preexisting FN matrices (Bourdoulous et al., 1998) or to stimulate increased FN matrix deposition (Yi and Ruoslahti, 2001), depending upon its concentration. In the present study, the III1H-mediated increases in cell growth and contraction occurred in the absence of any endogenous FN. These results indicate that, in addition to its ability to affect cellular events by altering matrix composition, the III1 module of FN can also directly affect cell function.

Sottile et al. (2000) recently demonstrated that HSPGs play a role in the stimulation of cell growth induced by FN polymerization. Similarly, in the present study, the stimulation of cell growth by GST–III1H,8–10 was inhibited by either heparin or pretreatment of cells with heparinase. In addition, hep-

arinase inhibited the localization of both GST–III1H,2–4 and intact FN to caveolae. These data suggest that HSPGs function as the cell surface receptor for the heparin-binding region of III1 and further, that a similar HSPG-dependent mechanism is involved in the partitioning of III1H and matrix FN into caveolae. Previous studies have localized the stress fiber–promoting activity of the COOH-terminal heparin-binding domain of FN to III13 (Bloom et al., 1999). In the present study, GST–III8–10,13 was unable to increase cell growth or contraction and did not localize to caveolae. However, addition of excess GST–III12–13 to cells inhibited GST–III1H,8–10-stimulated growth, suggesting that III13 can compete with III1H for binding to the glycosaminoglycan chains of the HSPGs. Additional interactions, possibly involving the core protein of the HSPG (Woods, 2001), likely contribute to the subsequent generation of distinct intracellular signals that modulate cell growth and contraction.

The molecular processing of information received by cells from their extracellular environment occurs in specific membrane domains, including caveolae, focal adhesions, and areas of cell–cell contact. Caveolae exist as cholesterol- and sphingolipid-enriched microdomains within the cell membrane and play a key role in signal transduction events (Brown and London, 1998). Several growth factor receptor tyrosine kinases as well as nonreceptor signaling proteins, including Src family kinases, MAPK, and PKCα, have been shown to localize to caveolae (Brown and London, 1998). The ability of heparin-binding III1 FN fragments, as well as matrix FN, to partition to caveolin-enriched microdomains represents a novel mechanism by which signals derived from the ECM may be transmitted to the interior of the cell to modulate growth and contractility.

During wound healing, migrating epithelial cells and fibroblasts deposit and remodel the ECM in order to support further cell ingrowth and neovascularization (Clark, 1995). Under normal circumstances, the synthesis of ECM proteins gradually decreases during tissue repair (Clark, 1995). However, in the absence of appropriate inhibitory signals, the synthetic phenotype of wound fibroblasts persists and can lead to the development of fibrotic changes within tissues, including excess deposition of FN, stimulation of fibroblast proliferation, and altered organization of collagen fibrils (Clark, 1995). As such, the continuous or inappropriate exposure of the matricryptic, heparin-binding activity of FN's III1 module may contribute to the fibrotic phenotype by enhancing and/or prolonging cell contraction and growth. Developing methods to control the extent and/or duration of the exposure of cells to matrix-specific epitopes may provide useful approaches to promote normal wound healing and prevent fibrosis.

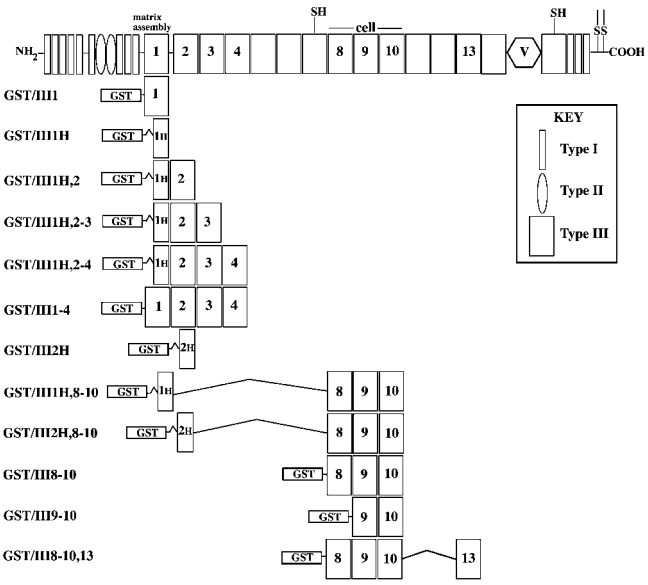

Figure 10. **FN fusion proteins.** Schematic representation of an FN subunit and recombinant GST fusion proteins. Relevant type III modules are numbered.

Materials and methods

Reagents

Human plasma FN was isolated from Cohn's fraction I and II, as previously described (Miekka et al., 1982). The NH_2-terminal 70-kD FN fragment was generated as previously described (Hocking et al., 1994). Vitronectin was purified from fibrinogen-depleted human plasma (Hocking et al., 1999). Unless otherwise indicated, chemical reagents were from Sigma-Aldrich.

Cell culture

Mouse embryo cells, derived from $FN^{-/-}$ embryos and adapted to grow under serum-free conditions (Sottile et al., 1998), were provided by Jane Sottile (University of Rochester, Rochester, NY). $FN^{-/-}$ cells were cultured on collagen-coated dishes in a 1:1 mixture of Cellgro® (Mediatech) and Aim V (Life Technologies).

Recombinant FNs

Fig. 10 illustrates the FN constructs used in this study. PCR was used to amplify human FN cDNA (a gift of Jean Thiery, Institut Curie, Paris, France) encoding the following amino acids (Petersen et al., 1989): a COOH-terminal fragment of the first type III module (III1H; bases 1802–2032; Ile 597–Thr 673), III1H plus the III2 module (III1H,2; bases 1802–2347; Ile 597–Thr 778), III1H plus the III2 and III3 modules (III1H,2–3; bases 1802–2635; Ile 597–Asp 874), III1H plus the III2, III3, and III4 modules (III1H,2–4; bases 1802–2905; Ile 597–Thr 964), the full-length first through fourth type III modules (III1–4; bases 1745–2905; Ser 578–Thr 964), a COOH-terminal fragment of the III2 module corresponding to the III1H fragment (III2H; bases 2132–2347; Val 707–Thr 778), the 8–10th type III modules (III8–10; bases 3716–4540; Ala 1326–Thr 1600), and the III13 module (III13; bases 5357–5623; Asn 1873–Thr 1961). The sense primer for III1H, III1H,2, III1H,2–3, and III1H,2–4 (5′-CCC**GGATCC**ATCCAGTGGAATGCACCACAG-3′), the sense primer for III1–4 (5′-CCC**GGATCC**AGTGGTCCTGTCGAAGTATTTAT-3′), and the sense primer for III2H (5′-CCC**GGATCC**GTCTCCTGGGTCTCAGCTTC-3′) contain a BamH1 site (shown in bold) at the 5′ end. The sense primer for III8–10 and III8–10,13 (5′-CCC**AGATCT**GCTGTTCCTCCTCCCACTGAC-3′) includes a BglII site. The sense primer for III13 (5′-CCC**ATCGAT**AATGTCAGCCCACCAAGAAGG-3′) includes a Cla site. The antisense primers for III1H (5′-CCC**GAATTC**CTATGTGCTGGTGCTGGTGGTG-3′), III1H,2 and III2H (5′-CCC**GAATTC**CTATGTTGTTTGTGAAGTAGACAGG-3′), III1H,2–3 (5′-CCC**GAATTC**CTAATCTGAGCGTGGGGTGCCAG-3′), and III1H,2–4 and III1–4 (5′-CCC**GAATTC**CTAGGTTGTCTGTTGAGCAGTCAG-3′) contain an EcoRI site. The antisense primers for III8–10 (5′-CCC**CCCGGG**CTATGTTCGGTAATTAATGGAAATTG-3′) and III8–10,13 (5′-CCC**CCCGGG**CTAAGTGGAGGCGTCGATGACCAC-3′) include a SmaI site. III1H,8–10 and III2H,8–10 were made by PCR amplification of either III1H or III2H with BamHI sites at both the 5′ and 3′ ends. The sense primers used were the same as those for III1H and III2H. The antisense primers for III1H (5′-CCC**GGATCC**TGTGCTGGTGCTGGTGGTG-3′) and III2H (5′-CCC**GGATCC**TGTTGTTTGTGAAGTAGACAGG-3′) contain BamHI sites. The III8–10 modules were PCR amplified with BglII and SmaI sites at the 5′ and 3′ ends, respectively. These restriction enzyme sites generate two additional amino acids (Gly and Ser) between either III1H or III2H and III8–10. To construct III8–10,13, an antisense primer for III10 (5′-CCC**ATCGAT**AATGTCAGCCCACCAAGAAGC-3′) was synthesized with a Cla site, which generates two additional amino acids (Ile and Asp) between III10 and III13. The III9–10 synergy site mutant ($GST/III9–10^{R1374,1379A}$) was produced using the following mutant primers: 5′-**GC**GGTGCCCCACTCT**GC**GAATTCCATCACCCTC-3′ (sense) and 5′-C**GC**AGAGTGGGGCACC**G**-

CATCTTCTCG-3′ (antisense). The outer primers were the same as those used to amplify nonmutant III9–10 (Hocking et al., 1999). The amplification of III1, III9–10, III12–13, and the heparin-binding domain of vitronectin have been previously described (Hocking et al., 1999). The PCR products were cloned into pGEX-2T (Amersham Biosciences) and transfected into DH5α bacteria (Sambrook et al., 1989). Proteins were isolated on glutathione-agarose (Amersham Biosciences) (Hocking et al., 1994). GST–III1 and GST–III1H were digested with TPCK-trypsin (Hocking et al., 1994). III1 was separated from GST by passing the digested material over SP-Sephadex C-25 (Amersham Biosciences). III1H was separated from GST by retention on heparin-Sepharose (Amersham Biosciences). GST–III8–10,13 bound to heparin-Sepharose and eluted at a concentration of 0.628 ± 0.009 M NaCl. By comparison, the 30-kD COOH-terminal heparin-binding FN fragment elutes at 0.63 M NaCl (Ingham et al., 1990).

Antibodies

Antibodies and their sources are as follows: anti-FN III1 IgG (9D2; Chernousov et al., 1991; a gift from Deane Mosher, University of Wisconsin, Madison, WI); mouse IgG (Cappel); anticaveolin polyclonal and LAMP-1 mAbs (BD Transduction Laboratories); anti-GST monoclonal and polyclonal IgG (Upstate Biotechnology); anti-vinculin mAb, anti–β-actin mAb, and anti-FN polyclonal IgGs (Sigma-Aldrich).

Growth assays

Growth assays were conducted as previously described (Sottile et al., 1998). For some experiments, recombinant FN constructs, nystatin, cyclodextrin, or heparinase I (5 mU/ml; Seikagaku Corp.) were added to collagen-adherent $FN^{-/-}$ cells 30 min before the addition of test proteins. Heparinase treatment was repeated every 24 h. After a 3- or 4-d incubation, cells were fixed, stained with crystal violet, and the absorbance at 590 nM was determined (Sottile et al., 1998).

Collagen gel contraction assays

Floating type I collagen gels were prepared as previously described (Hocking et al., 2000). Collagen gels imbedded with cells were incubated for 20 h and then removed from the wells and weighed. Collagen gel contraction was measured as a decrease in gel weight (Hocking et al., 2000). Data are reported as percent contraction: (1 − weight of the test gels/weight of gels not containing cells) × 100.

Solid-phase heparin binding assay

Glutathione-coated 96-well plates (Pierce Chemical Co.) were incubated with saturating concentrations of proteins (400 nM; 25 μg/ml GST–III8–10,13) in TBS with 0.5% Tween. Plates were then washed and incubated with heparin–albumin–biotin followed by HRP-NeutrAvidin (Pierce Chemical Co.). Parallel plates were incubated with a polyclonal anti-GST antibody followed by an HRP-conjugated goat anti–rabbit IgG (Bio-Rad Laboratories). The assay was developed using 2,2′-azino-bis (3-ethylbenzthiazoline sulfonic acid) and the absorbance at 405 nm was measured.

Statistical analysis

Data are expressed as mean ± SEM and represent one of at least three separate experiments performed in triplicate or quadruplicate. Significance was determined using one-way analysis of variance (ANOVA) or the *t* test for unpaired samples. Differences <0.05 were considered significant.

Immunofluorescence microscopy

Collagen-adherent $FN^{-/-}$ cells were incubated for 5 h with 250 nM of the GST fusion proteins. For inhibition studies, cells were pretreated for 0.5 h with 2.5 μg/ml filipin III or an equal volume of ethanol, 5 mU/ml heparinase I (Seikagaku Corp.), 100 mU/ml chondroitinase ABC (Seikagaku Corp.), 25 U/ml neuraminidase (Calbiochem-Novabiochem), or an equal volume of DME. In other experiments, $FN^{-/-}$ cells were seeded on coverslips coated with 10 μg/ml vitronectin, grown to confluence, and then incubated with 40 nM FN for 5 h. Cells were fixed with 2% paraformaldehyde and permeabilized with 0.5% Triton X-100. Fusion proteins were visualized using either anti-GST monoclonal or polyclonal antibodies. After staining, cells were examined with an Olympus BX60 microscope equipped with epifluorescence and photographed using a Spot digital camera.

Low-density membrane fractions

Low-density membrane fractions were prepared by extraction with either 1% Triton X-100 or 0.5 M sodium carbonate, pH 11.0 (Schwab et al., 2000). Confluent $FN^{-/-}$ cells were treated with 5 mU/ml heparinase I for 1 h before the addition of either 250 nM GST–III1H,2–4 or 40 nM FN for an additional 5 h. Two 150-mm dishes were used for each condition. Cells were washed with PBS and scraped into 2 ml of 1% Triton X-100 in MES-buffered saline (MBS; 25 mM MES, 150 mM NaCl, pH 6.5). In some studies, $FN^{-/-}$ cells were treated with 40 nM FN in the presence of either 25 μg/ml of 9D2 IgG or mouse IgG. After an 18-h incubation, cells were washed and scraped into 2 ml of 0.5 M sodium carbonate, pH 11. 2 ml of cell lysate was mixed with 2 ml of 80% sucrose in MBS. Samples were placed in a centrifuge tube and overlaid with 4 ml each of 30 (Triton extraction) or 35% (carbonate extraction) sucrose followed by 5% sucrose in MBS. Samples were centrifuged at 200,000 *g* at 4°C for 15 h. Sequential 1-ml fractions were collected and aliquots were analyzed by PAGE and immunoblotting.

Immunoblotting

PAGE and immunoblotting were performed as previously described (Hocking et al., 2000). Gel samples were reduced with 2% β-mercaptoethanol. Immunoblots were incubated with primary antibody in TBS-T (20 mM Tris, pH 7.6, 137 mM NaCl, 0.1% Tween 20) containing 1% BSA followed by a goat anti–rabbit, –mouse, or –rat HRP-linked secondary antibody. Blots were developed using ECL (Amersham Biosciences). After detection, blots were stripped by incubation with 0.2 M glycine, 0.1% SDS, 1% Tween, pH 4.0 (Miller et al., 1997). Blots were then washed, reblocked, and reprobed.

The authors thank Dr. Jane Sottile for providing the $Fn^{-/-}$ cells and valuable advice, and Dr. Ingrid Sarelius (University of Rochester) for assistance with the statistical analyses.

This work was supported by grants HL60181 and HL64074 from the National Institutes of Health.

Submitted: 10 December 2001
Revised: 20 May 2002
Accepted: 24 May 2002

References

Anderson, R.G.W. 1998. The caveolae membrane system. *Annu. Rev. Biochem.* 67: 199–225.

Aota, S., M. Nomizu, and K.M. Yamada. 1994. The short amino acid sequence Pro-His-Ser-Arg-Asn in human fibronectin enhances cell-adhesive function. *J. Biol. Chem.* 269:24756–24761.

Bloom, L., K.C. Ingham, and R.O. Hynes. 1999. Fibronectin regulates assembly of actin filaments and focal contacts in cultured cells via the heparin-binding site in repeat III_{13}. *Mol. Biol. Cell.* 10:1521–1536.

Bourdoulous, S., G. Orend, D.A. MacKenna, R. Pasqualini, and E. Ruoslahti. 1998. Fibronectin matrix regulates activation of RHO and CDC42 GTPases and cell cycle progression. *J. Cell Biol.* 143:267–276.

Brown, D.A., and E. London. 1998. Functions of lipid rafts in biological membranes. *Annu. Rev. Cell Dev. Biol.* 14:111–136.

Chernousov, M.A., F.J. Fogerty, V.E. Koteliansky, and D.F. Mosher. 1991. Role of the I-9 and III-1 modules of fibronectin in formation of an extracellular matrix. *J. Biol. Chem.* 266:10851–10858.

Clark, R.A.F. 1995. Wound repair. *In* The Molecular and Cellular Biology of Wound Repair. R.A.F. Clark, editor. Plenum Press, New York. 3–50.

Davis, G.E., K.J. Bayless, M.J. Davis, and G.A. Meininger. 2000. Regulation of tissue injury responses by the exposure of matricryptic sites within extracellular matrix molecules. *Am. J. Pathol.* 156:1489–1498.

Hocking, D.C., J. Sottile, and P.J. McKeown-Longo. 1994. Fibronectin's III-1 module contains a conformation-dependent binding site for the amino-terminal region of fibronectin. *J. Biol. Chem.* 269:19183–19191.

Hocking, D.C., J.S. Sottile, T. Reho, R. Fassler, and P.J. McKeown-Longo. 1999. Inhibition of fibronectin matrix assembly by the heparin-binding domain of vitronectin. *J. Biol. Chem.* 274:27257–27264.

Hocking, D.C., J. Sottile, and K.J. Langenbach. 2000. Stimulation of integrin-mediated cell contractility by fibronectin polymerization. *J. Biol. Chem.* 275: 10673–10682.

Hynes, R.O. 1990. Fibronectins. Springer-Verlag New York Inc., New York. 546 pp.

Ingham, K.C., S.A. Brew, and D.H. Atha. 1990. Interaction of heparin with fibronectin and isolated fibronectin domains. *Biochem. J.* 272:605–611.

Jockusch, B.M., P. Bubeck, K. Giehl, M. Kroemker, J. Moscher, M. Rothkegel, M. Rudiger, K. Schluter, G. Stanke, and J. Winkler. 1995. The molecular architecture of focal adhesions. *Annu. Rev. Cell Dev. Biol.* 11:379–416.

Keller, P., and K. Simons. 1998. Cholesterol is required for surface transport of influenza virus hemagglutinin. *J. Cell Biol.* 140:1357–1367.

Litvinovich, S.V., V.V. Novokhatny, S.A. Brew, and K.C. Ingham. 1992. Reversible unfolding of an isolated heparin and DNA binding fragment, the first type III module from fibronectin. *Biochim. Biophys. Acta.* 1119:57–62.

Magnusson, M., and D.F. Mosher. 1998. Fibronectin: structure, assembly, and cardiovascular implications. *Arterioscler. Thromb. Vasc. Biol.* 18:1363–1370.

Miekka, S.I., K.C. Ingham, and D. Menache. 1982. Rapid methods for isolation of human plasma fibronectin. *Thromb. Res.* 27:1–14.

Miller, T.M., M.G. Tansey, E.M. Johnson, Jr., and D.J. Creedon. 1997. Inhibition of phosphatidylinositol 3-kinase activity blocks depolarization- and insulin-like growth factor I-mediated survival of cerebellar granule cells. *J. Biol. Chem.* 272:9847–9853.

Morla, A., Z. Zhang, and E. Ruoslahti. 1994. Superfibronectin is a functionally distinct form of fibronectin. *Nature.* 367:193–196.

Pasqualini, R., S. Bourdoulous, E. Koivunen, V.L. Woods, and E. Ruoslahti. 1996. A polymeric form of fibronectin has antimetastatic effects against multiple tumor types. *Nat. Med.* 2:1197–1203.

Petersen, T.E., K. Skorstengaard, and K. Vibe-Pedersen. 1989. Primary structure of fibronectin. *In* Fibronectin. D.F. Mosher, editor. Academic Press, New York. 1–24.

Sambrook, J., E.F. Fritsch, and T. Maniatis. 1989. Plasmid vectors. *In* Molecular Cloning: A Laboratory Manual. Cold Spring Harbor Laboratory Press, Cold Spring Harbor, NY. 1.74–1.84.

Schwab, R.B., T. Okamoto, P.E. Scherer, and M.P. Lisanti. 2000. Analysis of the association of proteins with membranes. *In* Current Protocols in Cell Biology. J.S. Bonifacino, M. Dasso, J.B. Harford, J. Lippincott-Schwartz, and K.M. Yamada, editors. John Wiley and Sons, Inc., New York. 5.4.8–5.4.11.

Sechler, J.L., and J.E. Schwarzbauer. 1998. Control of cell cycle progression by fibronectin matrix architecture. *J. Biol. Chem.* 273:25533–25536.

Sechler, J.L., and J.E. Schwarzbauer. 1999. Fibronectin fibrillogenesis: a paradigm for extracellular matrix assembly. *Curr. Opin. Cell Biol.* 11:622–627.

Sottile, J., D.C. Hocking, and P.J. Swiatek. 1998. Fibronectin matrix assembly enhances adhesion-dependent cell growth. *J. Cell Sci.* 111:2933–2943.

Sottile, J., D.C. Hocking, and K.J. Langenbach. 2000. Fibronectin matrix assembly stimulates cell growth by RGD-dependent and -independent mechanisms. *J. Cell Sci.* 113:4287–4299.

Tellier, M.C., G. Greco, M. Klotman, A. Mosoian, A. Cara, W. Arap, E. Ruoslahti, R. Pasqualini, and L.M. Schnapp. 2000. Superfibronectin, a multimeric form of fibronectin, increases HIV infection of primary $CD4^+$ T lymphocytes. *J. Immunol.* 164:3236–3245.

Woods, A. 2001. Syndecans: transmembrane modulators of adhesion and matrix assembly. *J. Clin. Invest.* 107:935–941.

Yi, M., and E. Ruoslahti. 2001. A fibronectin fragment inhibits tumor growth, angiogenesis, and metastasis. *Proc. Natl. Acad. Sci. USA.* 98:620–624.

Zhong, C., M. Chrzanowska-Wodnicka, J. Brown, A. Shaub, A.M. Belkin, and K. Burridge. 1998. Rho-mediated contractility exposes a cryptic site in fibronectin and induces fibronectin matrix assembly. *J. Cell Biol.* 141:539–551.